Evidence for the priming effect in a planktonic estuarine microbial community

Andrew D. Steen*

Department of Earth and Planetary Sciences, University of Tennessee - Knoxville

Lauren N. M. Quigley and Alison Buchan

Department of Microbiology, University of Tennessee - Knoxville

November 6, 2015

Abstract

The 'priming effect', in which addition of labile carbon and/or nutrients changes remineralization rates of recalcitrant organic matter, has been intensively studied in soils, but is less well-documented in aquatic systems. We investigated the extent to which additions of nutrients or labile organic carbon could influence remineralization rates of microbially-degraded, recalcitrant ^{14}C-labeled phytoplankton necromass in microcosms inoculated with microbial communities drawn from Groves Creek Estuary in coastal Georgia, USA. We found that amendment with labile protein plus phosphorus increased recalcitrant organic carbon mineralization rates by up to 100%, whereas acetate slightly decreased mineralization rates relative to an unamended control. Addition of ammonium and phosphate induced a smaller effect, whereas addition of ammonium alone had no effect. Counterintuitively, alkaline phosphatase activities increased in response to the addition of protein under P-replete conditions, indicating that production of enzymes unrelated to the labile priming compound may be a mechanism for the priming effect. The observed priming effect was transient: after 36 days of incubation roughly the same quantity of organic carbon had been mineralized in all treatments including no-addition controls. This timescale suggests that priming in coastal systems does not influence the long-term preservation of organic carbon, but may influence the exchange of organic carbon between fresh waters, estuaries, and the coastal ocean.

*corresponding author: asteen1@utk.edu

1 Introduction

The 'priming effect' refers to changes in the remineralization rate of recalcitrant organic matter due to nonlinear interactions among substances in the environment (Kuzyakov et al., 2000). Although this effect has been the subject of intensive study in soils, it has only recently begun to attract substantial attention in aquatic systems (Guenet et al., 2010; Bianchi, 2011). Among aquatic systems, the priming effect may be particularly relevant in estuaries, where labile organic matter (OM, for instance autochthonous production) mix with more recalcitrant OM, such as aged terrestrial OM and recalcitrant marine OM (Guenet et al., 2010). Despite the voluminous evidence for the priming effect in soils (Kuzyakov, 2010), the evidence for priming in aquatic systems is more ambiguous. Several studies using unlabeled additions of labile organic matter to aquatic ecosystems showed by mass balance that additions of labile OM must have stimulated oxidation of more recalcitrant OM (De Haan, 1977; Shimp and Pfaender, 1985; Carlson et al., 2002; Farjalla et al., 2009; Hansell and Carlson, 2013); other investigators in freshwater environments have not found evidence for the priming effect (Bengtsson et al., 2014; Catalán et al., 2015). With the exception of Farjalla et al. (2009), which concerns a tropical lagoon, these studies were not performed in estuaries. Perhaps more importantly, the priming effect refers to changes in remineralization of recalcitrant OM in response to the addition of more labile OM and/or nutrients. It can be challenging to distinguish remineralization of labile versus recalcitrant OM using a mass-balance approach, in which only total fluxes of CO_2 are measured, because these approaches do not distinguish between oxidation of pre-existing, recalcitrant OM and added labile OM. Here we report the results of microcosm incubations to assess the extent to which additions of labile OM (as either acetate or bovine serum albumin, a protein) or nutrients (N and/or P) influenced the remineralization rates of biodegraded phytoplankton necromass by a surface water microbial community collected from a temperate coastal estuary (Grove's Creek, Georgia, USA). Phytoplankton were labeled with ^{14}C so fluxes of $^{14}CO_2$ derived from phytoplankton necromass could unambiguously be distinguished from unlabeled CO_2 derived from labile carbon. Periodic measurements of cell abundance, extracellular enzyme activities, and dissolved organic matter (DOM) fluorescence provided insight into the mechanisms of interactions between labile OM, nutrients, and phytoplankton necromass. These microcosms provided a tractable experimental system in which to determine whether the priming effect may plausibly influence remineralization rates of recalcitrant OM in estuaries.

2 Materials and Methods

2.1 Generation of ^{14}C-labeled organic matter

The marine phytoplankter Synechococcus sp. strain CB0101 was grown on SN15 medium (750 mL filtered seawater, 250 mL distilled water, 2.5 mL 3.53

M $NaNO_3$, 2.6 mL 352 mM K_2HPO_4, 5.6 mL 342 mM $Na_2EDTA \cdot 2\,H_2O$, 2.6 mL 37.7 mM Na_2CO_3, 1 mL 737 M cobalamin, 1 mL cyano trace metal solution [400 mL distilled water, 100 mL 297 mM citric acid$*H_2O$, 100 mL 229 mM ferric ammonium citrate, 100 mL 27 mM $MnCl_2 \cdot 4\,H_2O$, 100 mL 17.8 mM $Na_2MoO_4 \cdot 2\,H_2O$, 100 mL 859 µM $Co(NO_3)_2 \cdot 6\,H_2O$, 100 mL 7.7 mM $ZnSO_4 \cdot 7\,H_2O$]) in a sealed, 4-liter flask in the presence of 0.5 mCi $NaH^{14}CO_3^-$ (MP Biomedicals, Santa Ana, CA) under artificial illumination on a 12-hr/12-hr cycle at 28^{o}C. Stationary phase cultures were collected on 0.22 µM Supor filters (Pall Corporation, Port Washington, NY) and resuspended in artificial seawater (ASW) (Sigma Sea Salts, 20 g/L [Sigma-Aldrich, St. Louis, MO]), pH 8.1. A microbial community inoculum (collected at Bogue Sound, NC, from the dock of the Institute of Marine Sciences, University of North Carolina-Chapel Hill) was added to the phytoplankton biomass at 1% v/v and incubated in the dark at room temperature for 45 days. During the course of the incubation, the quantity of $O^{14}C$ was periodically measured using a Perkin-Elmer TriCarb 2910-TR liquid scintillation analyzer (Perkin-Elmer, Waltham, MA). The concentration of remaining OC was calculated by assuming the specific activity of phytoplankton-derived OC was equal to the specific activity of $DI^{14}C$ in the growth medium.

Phytoplankton OC decay was assumed to follow first-order kinetics:

$$OC_t = OC_0 e^{-kt} \tag{1}$$

where OC_t is the concentration of organic carbon at time t, OC_0 is the initial concentration of organic carbon, and k is the decay rate constant. k was determined from a nonlinear least squares regression of the OC concentration data to equation 1, and half-life was calculated as $t_{1/2} = ln(2)/k$. At the end of this initial degradation phase, ^{14}C-POM was collected by filtration (0.22 µm), resuspended in ASW (salinity = 20) and heat killed by boiling for 5 min. The POM was allowed to return to room temperature and added to the microcosms as described below.

2.2 Microcosm incubations

Microcosms containing 1 mM $PO^{14}C$ were established using combinations of labile carbon, in the form of sodium acetate or protein (bovine serum albumin [BSA]), phosphorus as phosphate, and/or nitrogen as ammonium. The labile carbon, N, and P were added at final concentrations of 500 µM-C, 75 µM-N, and 4.7 µM-P, respectively. BSA contains both C and N, at a ratio of 6.6 C:N. Thus, the concentration of inorganic N added to select microcosms was chosen to match this ratio. The P concentration was selected based on the Redfield ratio for N:P of 16. The treatments were as follows: (1) sodium acetate (250 µM acetate or 500 µM-C); (2) protein plus P (500 µM-C as BSA, 75 µM-N as BSA, 4.7 µM K_2HPO_4); (3) N (75 µM NH_4Cl); (4) N plus P (75 µM NH_4Cl, 4.7 µM- K_2HPO_4); and (5) control treatment with no C, N or P addition.

Microcosms were constructed as follows: the natural microbial community was obtained by pre-filtering a sample of estuarine water (from Skidaway Is-

land, Georgia) using a Whatman GF/A filter (Whatman, GE Healthcare Biosciences Corporation, Piscataway, NJ; nominal pore size 1.6 μm) to reduce grazer abundance. Prefiltered estuarine water was then filtered onto a 0.22 μm filter (Supor-200 Pall Corp, Ann Arbor, MI). Cells captured on the second filter were resuspended into artificial seawater (Sigma Sea Salts, 15.0 g/L). The cell suspension was mixed and then 3.9 mL was dispensed into master mixes for each treatment with 383 mL artificial seawater (15.0 g/L, adjusted to pH 8.1) for a targeted cell density of 10^6cells ml^{-1}. C, N and P were added to the master mixes as appropriate for each treatment, and PO14C (0.3779 μCi/ 1 mg $PO^{14}C$) was added to each master mix for a final concentration of 1 mM OC. 65 mL of each master mix was dispensed after gentle mixing into five replicate, 125 mL serum vials and capped with gastight butyl stoppers (National Scientific Supply, Rockwood, TN). The microcosms were then incubated in an incubator at 25 ^{o} C in the dark.

2.3 ^{14}C measurements

Throughout the course of the first 36 days of incubation, samples were collected to monitor the concentrations of total ^{14}C labeled organic carbon ($O^{14}C$), particulate organic carbon ($PO^{14}C$) and dissolved inorganic carbon ($DI^{14}C$). Total $O^{14}C$ was measured on days 0, 1, 2, 3, 6, 8, 10, 14, 17, 20, 22, 27, 30 and 36; $PO^{14}C$ was measured on days 0, 1, 2, 8, 14, 22, 30 and 36; and $DI^{14}C$ was measured on days 1, 2, 3, 6, 8, 10, 14, 17, 20, 22, 27, 30 and 36. In all cases, 0.5 ml samples were collected from serum vials using a 22.5-guage needle and a 1 ml syringe. To quantify total $O^{14}C$, the sample was added to a 20 ml scintillation vial preloaded with 50 μL of 10% H_2SO_4, to drive off $^{14}CO_2$. Samples were allowed to degas for 15 minutes in a fume hood. Finally, 5 ml of Ecoscint scintillation cocktail (National Diagnostics, Mississauga, OH) was added to each serum vial. To quantify $PO^{14}C$, the samples were filtered through a 0.22 μm filter polycarbonate filter (Millipore, Billerica, MA). The filters were added to scintillation vials containing 5 mL of scintillation fluid. To quantify $DI^{14}C$, samples were initially stored with 50 μL of 1 M NaOH. Just prior to measurement with a Perkin-Elmer TriCarb 2910-TR scintillation counter, samples were acidified by the addition of 0.5 mL of 0.2 M HCl. CO_2 was trapped by bubbling a stream of air through the sample into a 20 mL scintillation vial with a Teflon-septum cap containing 10 mL modified Woellers solution (50% scintillation fluid/50% β-phenylethylamine) for 20 minutes (Steen et al., 2012) . Tests with $NaH^{14}CO_3$ standards indicated $^{14}CO_2$ trapping efficiency was at least 95%. For all scintillation measurements, vials were vortexed, allowed to 'rest' for 24-72 hours, and vortexed again prior to measurement in order to minimize particle-induced quenching.

2.4 Modeling ^{14}C data

Total $O^{14}C$ and $PO^{14}C$ data were modeled assuming a reactive fraction, which decayed according to first-order kinetics, plus an unreactive fraction, in accor-

dance with Eq. 1:

$$OC_t = (OC_0 - R)\, e^{-kt} + R \tag{2}$$

where OC_t is the concentration of total OC or POC at time t, OC_0 is the initial total OC or POC concentration, R is the concentration of recalcitrant OC or POC (modeled here as totally unreactive, in contrast with the way the term is used elsewhere in this paper), k is the first-order degradation rate constant, and t is the incubation time. These models were fit to the data using nonlinear least squares regressions, with k and R as fitted parameters and OC_0 as a constant determined from measurements of the source phytoplankton (960 μM-C for total OC, 926 μM-C for POC). CO_2 production was modeled similarly (Eq. 3), assuming that the only source of $^{14}CO_2$ was the remineralization of recalcitrant $O^{14}C$.

$$CO_{2t} = A\left(1 - e^{-kt}\right) \tag{3}$$

95% confidence intervals were calculated using a Monte Carlo algorithm as implemented in the `propagate` R package. For the CO_2 data, priming at time t was defined as

$$p_t = \frac{\Sigma CO_{2treatment,t}}{\Sigma CO_{2control,t}} - 1 \tag{4}$$

Because observed $^{14}CO_2$ concentrations were non-normally distributed and temporally autocorrelated, a custom permutation test was used to test the null hypothesis that observed priming in each experimental treatment on each day was indistinguishable from zero (see R code in supplemental information).

2.5 Potential extracellular enzyme activities

Activities of three different extracellular enzymes were assayed during the course of the incubations on days 0 (3 hours after the start of incubations), 7, 16, 21, 29 and 35. β-glucosidase was assessed using 4-methylumbelliferyl-β-D-glucopyranoside (MUB-β-glu; Sigma-Aldrich, St. Louis, MO) at a final concentration of 200 μM. Leucyl aminopeptidase was assessed using L-leucine-7-amido-4-methylcoumarin (Leu-AMC; Chem-Impex International Inc., Wood Dale, IL) at a final concentration 400 μM. Alkaline phosphatase was assessed using 4-methylumbelliferyl phosphate (MUB−PO_4; Chem-Impex International Inc, Wood Dale, IL) at a final concentration 50 μM. At each measurement timepoint, 0.5 ml of each sample was added to 0.5 ml artificial seawater buffer and a small volume of substrate (MUB-β-glu: 20 μL, Leu-AMC: 20 μL, MUB-PO4: 50 μL). Cuvettes were capped and shaken and incubated at 22 ^{o}C. Fluorescence was periodically measured using a QuantiFluor ST single-cuvette fluorimeter over the course of approximately 2 hours as described in (Steen and Arnosti, 2013). Fluorescence values were calibrated with 4-methylumbelliferone and 7-amido-4-methylcoumarin as appropriate, and were analyzed using the enzalyze package for analysis of enzyme kinetics in R, available at http://github.com/adsteen/enzalyze.

2.6 Cell counts

Cell densities were assessed on days 1, 3, 6, 10, 14, 17, 20, 22, 27, 30, 36 and 57 days by microscopic direct counting following (Ortmann and Suttle, 2009). 0.5 mL of sample were taken from replicate A of each treatment and stored in cryovials. 10 µL of 25% filter-sterilized glutaraldehyde was added to the samples. Samples were stored at -80^{o}C. 100 µL of sample was added to 900 L of water. 50 µL of SYBR gold (25X) was added to each sample. Samples were incubated in the dark for 15 minutes. Stained samples were vacuum filtered through a 0.22 µm filter. The filter was removed and placed on a glass slide. 20 µL of anti-fade solution (480 µL 50% glycerol / 50% PBS; 20 µL p-phenylenediamine) was added on top of the filter on the slide before placing a cover slip on the slide. Bacteria were manually enumerated using a Leica CTR6000 microscope (Leica Microsystems, Buffalo Grove, IL).

2.7 Fluorescence spectroscopy of dissolved organic matter

Based on preliminary evidence that conditions in the treatments had begun to converge by 36 days, after 57 days we assessed the character of remaining DOM in selected samples using excitation-emission matrix (EEM) fluorescence spectroscopy. Due to the radioactive nature of the samples, fluorescence spectra were measured in sealed 1 cm $\times$ 1 cm methacrylate cuvettes (Fisher Scientific, Waltham, MA), which are advertised as transparent above 285 nm. In order to control for potential variability in optical properties among cuvettes, a Milli-Q water blank was measured in each cuvette prior to adding sample. For each measurement, a blank UV-vis absorbance scan was collected using Milli-Q water water on a Thermo Scientific Evolution 200 series spectrophotometer, and a blank fluorescence scan was collected on a Horiba Jobin Yvon Fluoromax 4 fluorescence spectrometer (Horiba Scientific, Kyoto, Japan). The excitation scan was from 240-450 nm in 5 nm increments, and the emission scan was from 250-550 nm in 2.5 nm increments. Finally, the Milli-Q water was removed from the cuvette, sample water was added and diluted 50% with Milli-Q water, and a sample fluorescence scan was collected using the same instrument settings. Sample 5B, which had an unacceptable blank, was discarded.

UV scans indicated that the methacrylate cuvettes began to absorb light below about 290 nm, so all excitation and emission wavelengths shorter than 295 nm were discarded. Sample fluorescence spectra were then corrected for inner-filtering effects, blank-subtracted, normalized to the appropriate days Raman spectrum, and masked for Raman and Rayleigh scattering.

BSA was the only fluorescent priming compound. For that reason, an initial fluorescence sample was taken from the control treatment prior to the addition of any priming compounds, and a separate initial sample was taken from the +BSA+P treatment to assess the fluorescence characteristics of the added BSA. Duplicate final samples were taken after 57 days incubation from each treatment.

EEMs data analysis techniques can be highly sensitive to the specific conditions under which fluorescence EEMs were measured (Cory et al., 2010). Since

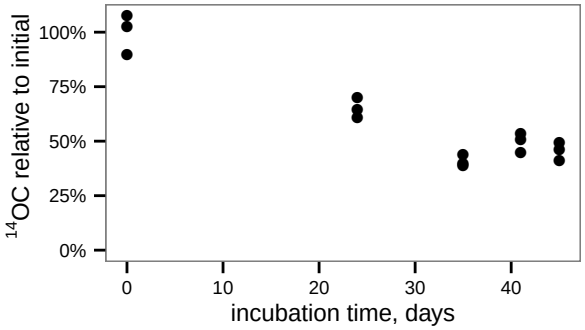

Figure 1: Degradation of ^{14}C-labeled phytoplankton necromass by an estuarine microbial community yields relatively recalcitrant, ^{14}C-labeled OM for use in microcosm experiments.

our EEMs were collected using a nonstandard cuvette type at a restricted set of wavelengths, we present the data qualitatively.

2.8 Data analysis

Data were analyzed using the R statistical platform (R Core Team, 2013) and visualized using the ggplot2 package (Wickham, 2009). All raw data and data-processing scripts are included as supplemental information.

3 Results

3.1 Character of ^{14}C-labeled phtoplankton necromass

To generate less-reactive organic matter for microcosm studies, a culture of the marine phytoplankton species Synecococcus sp. CB101 was first grown in the presence of ^{14}C -labeled bicarbonate. The labeled biomass was then subject to degradation by an estuarine microbial community for 45 days. At the end of the incubation period, 45 +/- 4 % of the initial phytoplankton O^{14}C remained (Fig. 1) consistent with a half-life for phytoplankton OC of 36 +/- 2 days based on a first-order decay kinetics.

3.2 Decay of total and particulate OC

Total ^{14}OC (i.e., D^{14}OC+P^{14}OC) and P^{14}OC decayed according to similar kinetics (Fig. 2). POC in the +BSA+P treatment decayed with a faster rate constant (0.62 +/- 0.46 day-1) than any other treatment (in the range of 0.06-0.19 day^{-1}, with error of 0.06-0.08 day^{-1}). Substantial noise in the data ob-

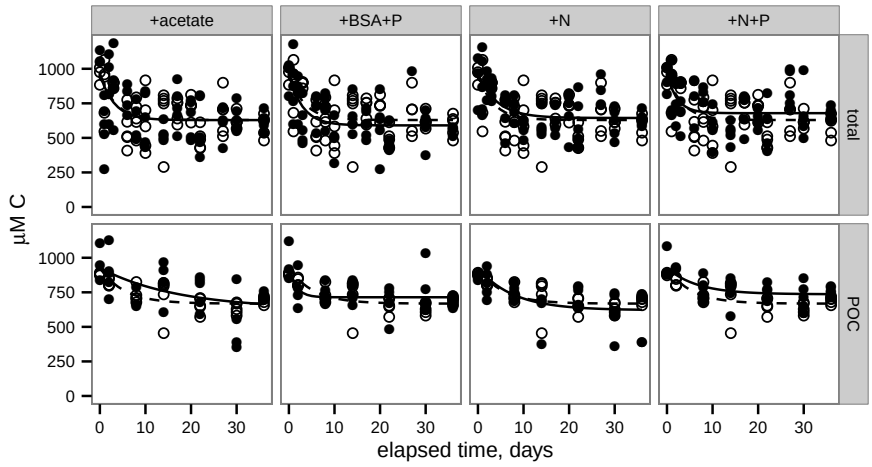

Figure 2: Remineralization of total OC (top row) and particulate OC (bottom row). Lines indicate the nonlinear least squares regressions to Eq. 2 (provided in Methods). Filled circles and solid lines indicate data from each treatment, as indicated across the top panels. Open circles and dashed lines indicate control data and are repeated in each panel for reference.

scured any other differences that might have existed in decay rate constant or concentrations of recalcitrant OM.

3.3 CO_2 production and priming

$^{14}CO_2$ production was faster in the +BSA+P treatment than in the control, indicating a positive priming effect which was distinguishable from zero ($p < 0.05$) from day 1 through day 21 (Fig 3; Table 1). The +N+P treatment also increased the rate of $^{14}CO_2$ production relative to control (Table 2). The rate constant for $^{14}CO_2$ production was also larger in the +N+P treatment than the control ($p < 0.05$) but the extent of priming in this treatment was never distinguishable from zero for an alpha of 0.05.

$^{14}CO_2$ production in the +acetate treatment was slightly slower than in the control, consistent with a negative or anti-priming effect; this effect was significant between day 14 and day 24, and the $^{14}CO_2$ production in the +N treatment was indistinguishable from the control. While the magnitude of anti-priming in the +acetate treatment was nearly constant throughout the incubation, positive priming in the +BSA+P treatment (and the +N+P treatments, if the observed priming in that treatment was not due to experimental error) was maximal at the first timepoint after labile organic matter was added, and decreased steadily thereafter. After 30-36 days of incubation, the total amount of $^{14}CO_2$ remineralized was indistinguishable among all treatments.

Test	Treatment	k, day^{-1}	R, μM C
total	+acetate	0.32 +/- 0.14	630 +/- 29
total	+BSA+P	0.33 +/- 0.11	590 +/- 25
total	+N	0.24 +/- 0.076	640 +/- 24
total	+N+P	0.44 +/- 0.2	680 +/- 22
total	control	0.3 +/- 0.12	630 +/- 24
POC	+acetate	0.058 +/- 0.059	630 +/- 140
POC	+BSA+P	0.62 +/- 0.46	710 +/- 21
POC	+N	0.13 +/- 0.063	620 +/- 41
POC	+N+P	0.15 +/- 0.077	740 +/- 23
POC	control	0.19 +/- 0.062	670 +/- 19

Table 1: Modeled rate constants (k) and recalcitrant organic carbon concentration (R) for total $O^{14}C$ and $PO^{14}C$ in each incubation. k and R were determined according to Eq. 2 (provided in the Methods).

Treatment	A, μM C	k, day^{-1}
+acetate	165 +/- 10.6	0.969 +/- 0.016
+BSA+P	185 +/- 7.9	0.2023 +/- 0.0287
+N	186 +/- 12.3	0.1001 +/- 0.017
+N+P	173 +/- 8.4	0.1741 +/- 0.028
control	185 +/- 10.0	0.1001 +/- 0.017

Table 2: Modeled asymptotes (A) and rate constants (k) for $^{14}CO_2$ production in each incubation.

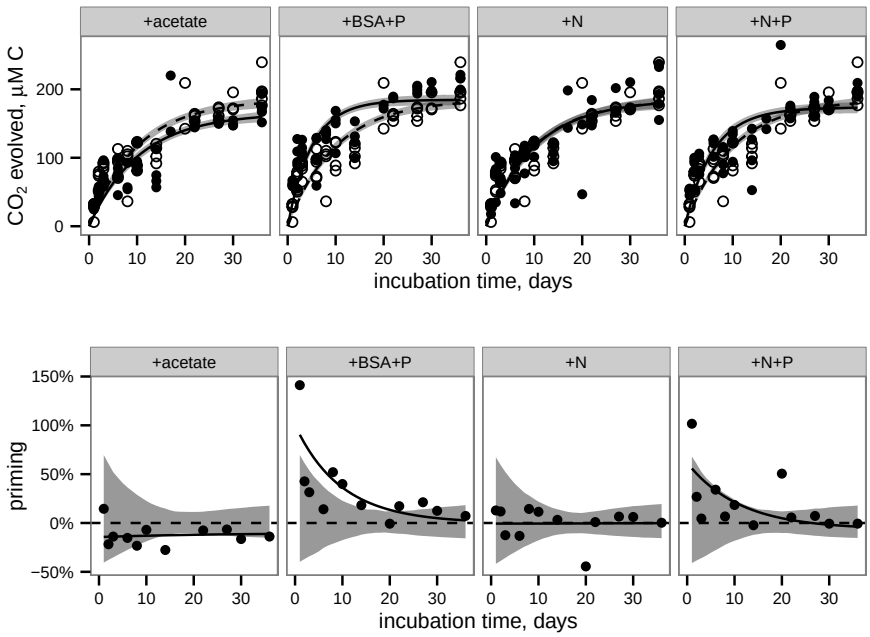

Figure 3: CO_2 production (top row) and priming (bottom row) in each treatment. Top row: Filled circles and solid indicate data from treatments. Open circles and dashed lines indicate data from the control (i.e., no added compounds) and are repeated in each panel for reference. Lines indicate best fits to Eq. 3 (provided in Methods). Shaded bands indicate standard error of the model fits estimated by a Monte Carlo technique. Bottom row: Priming, calculated according to Eq. 4 (provided in Methods). Circles indicate priming calculated from the average CO2 concentrations at each timepoint. Solid lines represent priming calculated from the fit lines shown in the top panel for each corresponding treatment. Shaded bands indicate the region that is indistinguishable from zero priming.

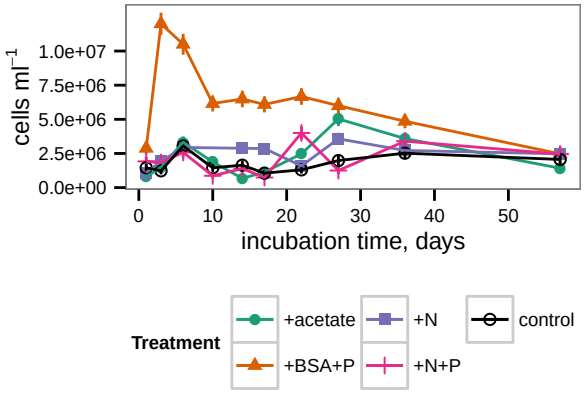

Figure 4: Cell abundance during the incubation. Error bars represent standard error of cell counts.

3.4 Cell abundance and extracellular enzymes

Cell abundances in the incubations increased from approx. 10^6 cells ml^{-1} in each treatment after 1 day of incubation to $1.4 - 2.5 \times 10^6$ cells ml^{-1} after 57 days of incubation, with relatively little difference among treatments (Fig 4). However, substantial differences among treatments occurred during the course of the incubation. In the +BSA+P treatment, cell densities quickly increased to a maximum of 1.2×10^7 cells ml $- 1$ after 3 days and then decreased steadily through the end of the incubation. Other treatments were characterized by an initial peak at 6 days incubation. Cell abundance in the +N treatment remained roughly constant after 6 days, whereas the control, +acetate, and +N+P treatments , followed by a minimum in cell abundance at approximately 17 days, and, in the case of the +acetate treatment, a second, larger peak in cell abundance at 27 days.

Potential activities of extracellular enzymes also varied as a function of both time and treatment (Fig 5). β-glucosidase activities were generally indistinguishable from zero throughout the incubation for all treatments. Leucyl aminopeptidase activities were far greater in the +BSA+P treatment than in any other treatment, although activities were significantly greater than zero in each treatment. The timecourse of leucyl aminopeptidase activities followed cell counts closely. Alkaline phosphatase activities were also greater in the +BSA+P treatment than in any other treatment, but the timecourse of activities followed a different path than the timecourse of cell counts: the maximum value was at 17 days rather than 6 days, and the peak in activities was less dramatic than either the peak in leucyl aminopeptidase activities or cell counts. While most measures of biological activity ceased at day 35 due to limited sample volume, a

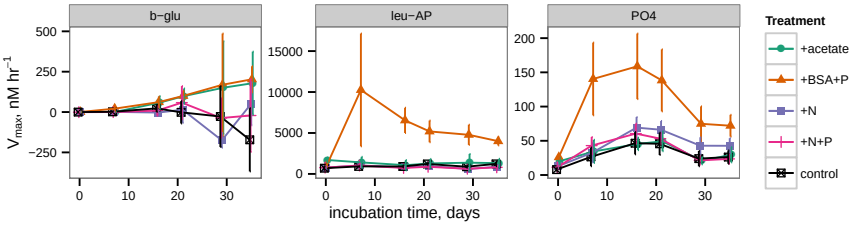

Figure 5: Potential extracellular enzyme activities during the incubation. b-glu represents β-glucosidase, leu-AP represents leucyl aminopeptidase, and PO4 represents alkaline phosphatase.

final measurement of cell density was made at day 57 and found to range from 1.4×10^6 cells ml^{-1} (+acetate treatment) to 2.5×10^6 cells ml^{-1} (+BSA+P, +N, +N+P treatments).

3.5 Chemical transformations of DOM

At the conclusion of the incubation period (day 57), the remaining sample volume was sacrificed for excitation-emission matrix (EEM) fluorescence spectroscopic analysis and compared with samples preserved from the first day of the incubation. The intensity of the FDOM signal increased in all samples over the course of the incubation (Fig 6). The nature of the signal, as revealed by EEM, however, did not vary much by treatment, with the exception of the +BSA+P treatment. In this treatment, the protein peak from the added BSA (visible at the bottom of the panel for the initial +BSA+P treatment in Fig 4) dominated the phytoplankton recalcitrant OM signal. By the end of the incubation, however, there was no distinct protein signal, and the overall form of the EEM in the +BSA+P treatment was considerably more intense but similarly shaped to the signals from the other treatments.

4 Discussion

4.1 Reactivity of source $O^{14}C$

During the preparation of recalcitrant OM, the radiolabeled, phytoplankton-derived OM used in this experiment decayed with a pseudo-first order half-life of 36 +/- 2 days, consistent with semi-labile estuarine DOC (Raymond and Bauer, 2000). The phytoplankton-OM decay data here were too sparse to accurately model with a multi-G model (Fig. 1), but heterotrophic microbial activity rapidly converts fresh biomass into a complex mixture of compounds which is unreactive on a timescale of years via the 'microbial carbon pump' (Fry et al., 1996; Ogawa et al., 2001; Jiao et al., 2010). OM reactivity is typically defined along a broad spectrum from labile to recalcitrant. While we do not know

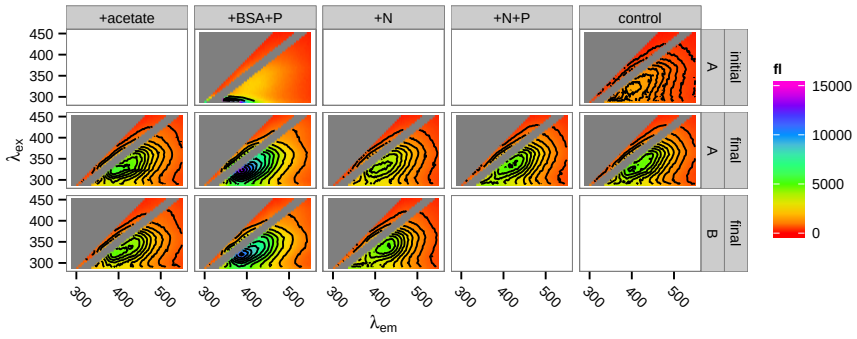

Figure 6: Fluorescence spectra of incubation DOM at the start and at the end of the incubations. Top row: spectra of the +BSA+P treatment and the control treatment at time zero ('initial'). Middle and bottom rows: replicate spectra after 57 days incubation ('final'). Insufficient sample remained for duplicate measurement of the +N+P and control samples after 57 days. 'A' and 'B' in the right-side panel labeled refer to incubation replicates.

the discrete chemical composition, nor the reactivity of individual components present in the phytoplankton-derived OM following the initial 45-day incubation period, this material is unquestionably less reactive than fresh phytoplankton OM. Therefore we refer to this material as 'recalcitrant'.

4.2 Role of P and labile organic C in recalcitrant OM mineralization

The results provide evidence of faster OM mineralization in the presence of added protein plus phosphate (+BSA+P treatment) and possibly added inorganic N and phosphate (+N+P), but not inorganic N alone (+N). These data suggest that heterotrophic metabolism of recalcitrant OM was limited in part by phosphorus. It is important to note that the factors limiting the remineralization of recalcitrant OM may differ from the factors limiting overall bacterial production. There was also a clear interaction between the form of N and P: the magnitude of early priming was about twice as large in the +BSA+P treatment as in the +N+P treatment. Consistent with reports from soils that addition of labile carbon without nutrients can induce microbial community shifts towards organisms specialized for mineralizing simple molecules (Fontaine et al., 2003), addition of acetate slowed the remineralization rate of the phytoplankton detritus. Thus, the magnitude and even direction of priming was influenced by both

the redox status of nutrients (organic versus inorganic) as well as the nature of organic carbon.

4.3 Priming as a transient effect

Recalcitrant OM was remineralized up to 100% faster in the +BSA+P treatment than in the control, but this effect was transient (Fig 3). After about 30 days, roughly the same amount of recalcitrant OM had been mineralized in each experiment. Cell densities (Fig 4) and enzyme activities (Fig 5) also converged towards the end of the experiment. Fluorescence spectroscopy indicated that, after 57 days of incubation, the composition of fluorescent DOM was indistinguishable among all treatments except for +BSA+P. In that treatment a large protein-like peak persisted at the end of the incubation, consistent with abiotic production of microbially unavailable protein(Keil and Kirchman, 1994) (Fig 6).

Interestingly, Catalán et al. (2015) recently found no evidence of priming in Swedish lakes. That study contained a very large number of experimental treatments, but only a single timepoint, after 35 days of incubation, whereas in the experiment reported here, priming effects were no longer observable after 21 - 24 days. The priming effect arises from interactions between disparate microorganisms and pools of organic carbon and nutrients (Blagodatskaya and Kuzyakov, 2008). Given the complexities of these interactions, it is likely that the magnitude, direction and timing of priming varies substantially among aquatic environments.

4.4 Mechanisms of priming

Cell abundances, leucyl aminopeptidase activity and phosphatase activity all increased substantially and rapidly in the +BSA+P treatment (Figs 4 and 6). These are consistent with a scenario in which cells grew rapidly using BSA as substrate, producing excess leucyl aminopeptidase, which acted on other protein-like components of the recalcitrant $O^{14}C$. Kuzyakov et al. (2000) cite changes in microbial biomass as a primary mechanism of priming in soils. Surprisingly, alkaline phosphatase activity also increased in the +BSA+P treatment, despite the substantial addition of P in that treatment. Some marine bacteria produce alkaline phosphatase constituitively (Hassan and Pratt, 1977), which may account for the observed increase in alkaline phosphatase activity in the +BSA+P treatment here. Alternatively, since the peak in phosphatase activity occurred at 17 days while cell abundance was declining, it is possible that the extracellular phosphatase enzymes may have been released from cytoplasm as cells lysed following the peak in cell abundance at day 3. In either case, the observed increase in the activity of phosphatase provides mechanistic support for the hypothesis that addition of one compound can spur hydrolysis of chemically unrelated compounds, thereby making them bioavailable. Many aquatic extracellular peptidases (protein-degrading enzymes) are relatively promiscuous

(Steen et al., 2015) which suggests that peptidases produced in order to degrade BSA likely hydrolyzed some fraction of the recalcitrant $O^{14}C$ as well.

4.5 Relevance to carbon processing in estuaries

Priming in this study was substantial but transient. The relevant priming timescale observed here of days-to-tens-of-days, coincides with typical hydrologic residence times of passive-margin estuaries (Alber and Sheldon, 1999). Priming in estuaries may therefore influence whether OC is remineralized in situ or exported to the coastal ocean.

Is the priming effect that we observed in microcosm incubations with defined substrate additions relevant to natural systems? In estuaries, degraded OM (e.g. terrestrial OM or dissolved remnants of coastal phytoplankton blooms) can come into contact with fresh DOC produced in situ (Raymond and Bauer, 2001). Marsh grasses exude substantial amounts of labile compounds, including acetate (Hines et al., 1994; Jones, 1998), and phytoplankton growing in estuaries likely also serve as a source of labile OM (Carlson and Hansell, 2015). Here, we have shown that estuarine microbial communities are capable of being 'primed' (or 'anti-primed') by the addition of labile OM and nutrients to mineralize recalcitrant OM more quickly. Inputs of labile carbon and nutrients may therefore influence fluxes of less reactive OM between estuaries and the coastal ocean.

References

M Alber and J E Sheldon. Use of a date-specific method to examine variability in the flushing times of Georgia estuaries. *Estuarine Coastal and Shelf Science*, 49(4):469–482, 1999. ISSN 02727714. doi: 10.1006/ecss.1999.0515. URL <Go to ISI>://000083566700002.

Mia M Bengtsson, Karoline Wagner, Nancy R Burns, Erik R Herberg, Wolfgang Wanek, Louis a Kaplan, and Tom J Battin. No evidence of aquatic priming effects in hyporheic zone microcosms. *Scientific reports*, 4:5187, 2014. ISSN 2045-2322. doi: 10.1038/srep05187. URL http://www.pubmedcentral.nih.gov/articlerender.fcgi?artid=4046132&tool=pmcentrez&rendertyp

T. S. Bianchi. The role of terrestrially derived organic carbon in the coastal ocean: A changing paradigm and the priming effect, 2011. ISSN 0027-8424.

. Blagodatskaya and Y. Kuzyakov. Mechanisms of real and apparent priming effects and their dependence on soil microbial biomass and community structure: critical review. *Biology and Fertility of Soils*, 45(2):115–131, oct 2008. ISSN 0178-2762. doi: 10.1007/s00374-008-0334-y. URL http://link.springer.com/10.1007/s00374-008-0334-y.

Craig A. Carlson and Dennis A. Hansell. DOM Sources, Sinks and Reactivity. In Dennis A. Hansell and Craig A. Carlson, editors, *Biogeochemistry of Marine Dissolved Organic Matter*, pages 66–126. Second edi edition, 2015. ISBN 978-0-12-405940-5.

Craig A. Carlson, Stephen J. Giovannoni, Dennis A. Hansell, Stuart J. Goldberg, Rachel Parsons, Mark P. Otero, Kevin Vergin, and Benjamin R. Wheeler. Effect of nutrient amendments on bacterioplankton production, community structure, and DOC utilization in the northwestern Sargasso Sea. *Aquatic Microbial Ecology*, 30(1):19–36, 2002.

Núria Catalán, Anne M Kellerman, Hannes Peter, Francesc Carmona, and Lars J Tranvik. Absence of a priming effect on dissolved organic carbon degradation in lake water. *Limnology and Oceanography*, 60(1): 159–168, jan 2015. ISSN 1939-5590. doi: 10.1002/lno.10016. URL http://dx.doi.org/10.1002/lno.10016.

Rose M. Cory, Matthew P. Miller, Diane M. McKnight, Jennifer J. Guerard, and Penney L. Miller. Effect of instrumentspecific response on the analysis of fulvic acid fluorescence spectra. *Limnology and Oceanography: Methods*, 8(2):67–78, feb 2010. ISSN 1541-5856. doi: 10.4319/lom.2010.8.67. URL http://onlinelibrary.wiley.com/doi/10.4319/lom.2010.8.67/abstract.

H. De Haan. Effect of benzoate on microbial decomposition of fulvic acids in Tjeukemeer (the Netherlands). *Limnology and Oceanography*, 22(1): 38–44, 1977. ISSN 00243590. doi: 10.4319/lo.1977.22.1.0038. URL http://doi.wiley.com/10.4319/lo.1977.22.1.0038.

Vinicius F Farjalla, Claudio C Marinho, Bias M Faria, André M Amado, Francisco de A Esteves, Reinaldo L Bozelli, and Danilo Giroldo. Synergy of fresh and accumulated organic matter to bacterial growth. *Microbial ecology*, 57(4): 657–66, may 2009. ISSN 1432-184X. doi: 10.1007/s00248-008-9466-8. URL http://www.ncbi.nlm.nih.gov/pubmed/18985269.

Sébastien Fontaine, André Mariotti, and Luc Abbadie. The priming effect of organic matter: A question of microbial competition? *Soil Biology and Biochemistry*, 35(6):837–843, 2003. ISSN 00380717. doi: 10.1016/S0038-0717(03)00123-8.

Brian Fry, Charles S Hopkinson, Amy Nolin, Bosse Norrman, and Ulla Li Zweifel. Long-term decomposition of DOC from experimental diatom blooms, 1996. ISSN 00243590.

B Guenet, M Danger, L Abbadie, and G Lacroix. Priming effect: bridging the gap between terrestrial and aquatic ecology. *Ecology*, 91(10): 2850–2861, 2010. ISSN 0012-9658. doi: 10.1890/09-1968.1. URL http://www.esajournals.org/doi/abs/10.1890/09-1968.1.

Dennis A. Hansell and Craig A. Carlson. Localized refractory dissolved organic carbon sinks in the deep ocean. *Global Biogeochemical Cycles*, 27 (3):705–710, sep 2013. ISSN 08866236. doi: 10.1002/gbc.20067. URL http://doi.wiley.com/10.1002/gbc.20067.

H M Hassan and D Pratt. Biochemical and physiological properties of alkaline phosphatases in five isolates of marine bacteria. *J. Bacteriol.*, 129(3):1607–1612, mar 1977. URL http://jb.asm.org/content/129/3/1607.short.

Mark E. Hines, Gary T. Banta, Anne E. Giblin, John E. Hobbie, and Joyce B. Tugel. Acetate concentrations and oxidation in salt-marsh sediments. *Limnology and Oceanography*, 39(1):140–148, 1994. ISSN 00243590. doi: 10.4319/lo.1994.39.1.0140. URL http://onlinelibrary.wiley.com/store/10.4319/lo.1994.39.1.0140/asset/lno19943910140.pdf?v=

Nianzhi Jiao, Gerhard J Herndl, Dennis a Hansell, Ronald Benner, Gerhard Kattner, Steven W Wilhelm, David L Kirchman, Markus G Weinbauer, Tingwei Luo, Feng Chen, and Farooq Azam. Microbial production of recalcitrant dissolved organic matter: long-term carbon storage in the global ocean. *Nature reviews. Microbiology*, 8(8):593–9, aug 2010. ISSN 1740-1534. doi: 10.1038/nrmicro2386. URL http://www.ncbi.nlm.nih.gov/pubmed/20601964.

David L. Jones. Organic acids in the rhizosphere - A critical review, 1998. ISSN 0032079X.

Richard G Keil and David L Kirchman. Abiotic transformation of labile protein to refractory protein in sea water. *Marine Chemistry*, 45(3):187–196, feb 1994. ISSN 03044203. doi: 10.1016/0304-4203(94)90002-7. URL http://linkinghub.elsevier.com/retrieve/pii/0304420394900027.

Y. Kuzyakov, J. K. Friedel, and K. Stahr. Review of mechanisms and quantification of priming effects, 2000. ISSN 00380717.

Yakov Kuzyakov. Priming effects: Interactions between living and dead organic matter. *Soil Biology and Biochemistry*, 42(9):1363–1371, sep 2010. ISSN 00380717. doi: 10.1016/j.soilbio.2010.04.003. URL http://www.sciencedirect.com/science/article/pii/S0038071710001355.

H Ogawa, Y Amagai, I Koike, K Kaiser, and R Benner. Production of refractory dissolved organic matter by bacteria. *Science (New York, N.Y.)*, 292(5518): 917–20, may 2001. ISSN 0036-8075. doi: 10.1126/science.1057627. URL http://www.ncbi.nlm.nih.gov/pubmed/11340202.

Alice C Ortmann and Curtis A Suttle. Determination of Virus Abundance by Epifluorescence Microscopy. In *Bacteriophages - Methods and Protocols, Volume 1: Isolation, Characterization, and Interactions*, volume 501, pages 87–95. 2009. ISBN 978-1-58829-682-5. doi: 10.1007/978-1-60327-164-6. URL http://www.springerlink.com/index/10.1007/978-1-60327-164-6.

R Core Team. R: A Language and Environment for Statistical Computing, 2013.

Peter A. Raymond and James E. Bauer. Bacterial consumption of DOC during transport through a temperate estuary. *Aquatic Microbial Ecology*, 22(1): 1–12, 2000. ISSN 09483055. doi: 10.3354/ame022001.

Peter A. Raymond and James E. Bauer. DOC cycling in a temperate estuary: A mass balance approach using natural 14C and 13C isotopes, 2001. ISSN 0024-3590.

Robert Shimp and Frederic K. Pfaender. Influence of Naturally Occurring Humic Acids on Biodegradation of Monosubstituted Phenols by Aquatic Bacteria. *Appl. Envir. Microbiol.*, 49(2):402–407, feb 1985. URL http://aem.asm.org/content/49/2/402.short.

Andrew D. Steen and Carol Arnosti. Extracellular peptidase and carbohydrate hydrolase activities in an Arctic fjord (Smeerenburgfjord, Svalbard. *Aquatic Microbial Ecology*, 69(2):93–99, 2013. ISSN 09483055. doi: 10.3354/ame01625. URL http://www.int-res.com/abstracts/ame/v69/n2/p93-99/.

Andrew D. Steen, Kai Ziervogel, Sherif Ghobrial, and Carol Arnosti. Functional variation among polysaccharide-hydrolyzing microbial communities in the Gulf of Mexico. *Marine Chemistry*, 138-139:13–20, jul 2012. ISSN 03044203. doi: 10.1016/j.marchem.2012.06.001. URL http://www.sciencedirect.com/science/article/pii/S0304420312000746.

Andrew D. Steen, Jasmine P. Vazin, Shane M. Hagen, Katherine H. Mulligan, and Steven W. Wilhelm. Substrate specificity of aquatic extracellular peptidases assessed by competitive inhibition assays using synthetic substrates.

Aquatic Microbial Ecology, 75(3):271–281, 2015. doi: 10.3354/ame01755. URL http://www.int-res.com/abstracts/ame/v75/n3/p271-281/.

Hadley Wickham. *ggplot2: Elegant Graphics for Data Analysis*. Springer, New York, 2009. URL http://books.google.com/books?id=rhRqtQAACAAJ&dq=intitle:ggplot2+inauthor:wickham&